Mon. Not. R. Astron. Soc. **343,** 47–55 (2003)

The interstellar medium local to HD 10125

S. Cichowolski,[1★†] E. M. Arnal,[1,2‡] C. E. Cappa,[1,2‡] S. Pineault[3] and N. St-Louis[4]

[1]*Instituto Argentino de Radioastronomía, CC no 5, 1894 Villa Elisa, Argentina*
[2]*Facultad de Ciencias Astronómicas y Geofísicas, Universidad Nacional La Plata 1900 La Plata, Argentina*
[3]*Département de Physique et Observatoire du Mont Mégantic, Université Laval, Ste-Foy, Québec, Canada G1K 7P4*
[4]*Département de Physique et Observatoire du Mont Mégantic, Université de Montréal, CP 6128, Succursale Centre Ville, Montréal, Québec, Canada H3C 3J7*

Accepted 2003 February 20. Received 2003 February 18; in original form 2002 May 30

ABSTRACT

Based on an H I line and 408- and 1420-MHz radio continuum survey carried out at the Dominion Radio Astrophysical Observatory (DRAO), the environment of the O star HD 10125 has been studied. In addition, complementary radio continuum images, as well as infrared data of the same region have been analysed. An arc-like structure is found in all the radio continuum data. From the 21-cm line data, an H I minimum is found in the velocity range −27 to −32 km s^{-1}. Although HD 10125 is not at the centre of the H I cavity, its eccentric position is consistent with the observed stellar proper motion. The H I cavity and the continuum arc-like structure show an excellent morphological correlation. The radio continuum emission has a spectral index ($S_\nu \sim \nu^\alpha$) $\alpha = 0.0 \pm 0.1$, which establishes the thermal nature of the arc-like feature. The dust temperature obtained from the infrared data is higher in the area where the continuum emission is present. A distance of 3 kpc is derived for the star, the H I cavity and the radio continuum structure. We conclude that all the features we have found are physically related to each other. The O star has enough energetic photons to both ionize the surrounding gas and heat up the dust and, through its powerful wind, also sweep up the H I and H II gas.

Key words: stars: individual: HD 10125 – ISM: bubbles – H II regions – infrared: ISM.

1 INTRODUCTION

The structure and dynamics of the interstellar medium (ISM) are strongly affected by the action of massive stars, not only at the end of their lives when they explode as supernovae, but also during the more stable phases of their evolution. Massive stars deposit in the ISM a huge number of ionizing photons and transfer to it vast amounts of mechanical energy via their powerful stellar winds. Consequently, massive stars create what is known as an *interstellar bubble*, i.e. a minimum in the gas distribution characterized by a low volume density ($n \sim 10^{-2}$–10^{-3} cm^{-3}) and a high temperature ($T \sim 10^{6-7}$ K), surrounded by an expanding envelope (Weaver et al. 1977). If the star is either at rest or has a low spatial velocity with respect to its local ISM, it should be seen projected on to, or close to, the centre of the H I minimum. Several models have been developed to describe the evolution of the structures created in the ISM as a consequence of the action of these stars (Avedisova 1972; Weaver et al. 1977).

Observationally, one possible way to study this interaction is by analysing the H I and H II gas distributions in the environment of these stars. The radiation emitted by hot, massive stars can be absorbed by the interstellar dust which is heated, so an analysis of the infrared emission is also useful. Several H I voids and shells have been found around massive stars (e.g. Cappa de Nicolau & Niemela 1984; Arnal 1992; Arnal et al. 1999; Cappa & Herbstmeier 2000; Cazzolato & Pineault 2000; Arnal 2001; Cichowolski et al. 2001). Since the angular resolution in those studies varies from ∼2 to 30–40 arcmin, it is impossible to make a meaningful comparison among the parameters of different H I cavities derived from observations carried out using quite dissimilar instruments. The Canadian Galactic Plane Survey (CGPS; Normandeau, Taylor & Dewdney 1997; Higgs 1999; Taylor 2001) is a high-resolution (∼1 arcmin) H I line and 408- and 1420-MHz radio-continuum survey of the Galactic plane carried out at the Dominion Radio Astrophysical Observatory (DRAO). It provides the unique opportunity of carrying out an unbiased homogeneous study of the ISM structures possibly associated with massive stars and their evolved descendants. In this paper we report on CGPS data towards the Galactic O star HD 10125.

HD 10125 is a star catalogued as an O9.5Ib by Münch (1957) and as an O9.7II by Walborn (1971) and is located at $(l, b) = (128.^\circ29, +1.^\circ82)$ or (α, δ) (J2000) $= (1^h40^m52.^s76, 64^\circ10'23.''1)$. Its distance is estimated to 2.7 kpc by Cruz-González et al. (1974), 3 kpc by Savage et al. (1985) and 3.4 kpc by Wakker et al. (1998). The proper motion of this star according to both the

★E-mail: silvina@iar.unlp.edu.ar
†Fellowship from CONICET, Argentina.
‡Member of Carrera del Investigador Científico, CONICET, Argentina.

Table 1. Observational parameters.

Parameter	Value
H I line:	
Synthesized beam	1.06×1.0 arcmin^2
Position angle[a]	72.°4
Observed rms noise (single channel) (K)	1.0
Bandwidth (MHz)	1.0
Channel separation (km s^{-1})	0.82
Velocity resolution (km s^{-1})	1.3
Central velocity (km s^{-1})	−60.0
Velocity coverage (km s^{-1})	211
1420 MHz:	
Synthesized beam	0.89×0.83 arcmin^2
Position angle[a]	73.°6
Observed rms noise (K)	0.06
Bandwidth (MHz)	30
408 MHz:	
Synthesized beam	3.02×2.84 arcmin^2
Position angle[a]	75.°5
Observed rms noise (K)	0.4
Bandwidth (MHz)	4.0

[a]Position angle measured counterclockwise from the longitude axis.

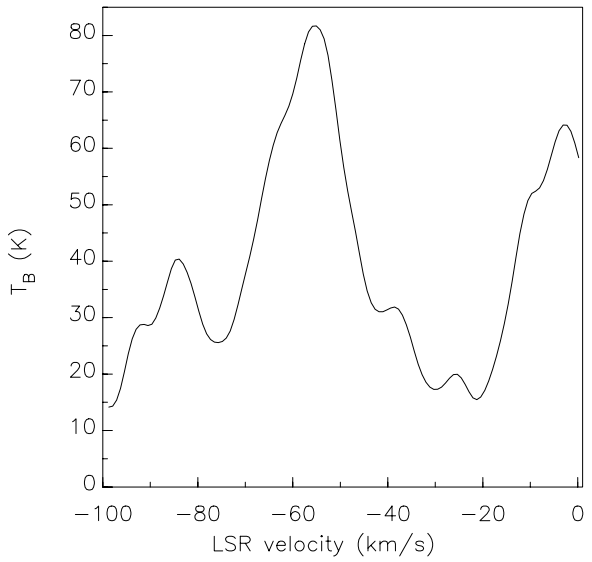

Figure 1. Average H I emission spectrum within a circle 50 arcmin in radius centred at the O star position.

Hipparcos Main Catalogue and the Tycho-2 Catalogue is (μ_α, μ_δ) (mas yr^{-1}) = (−1.70 ± 1.17, 1.10 ± 1.23) and (4 ± 1.6, 1.8 ± 1.6), respectively. Owing to a more advanced reduction technique, we shall adopt the Tycho-2 proper motions. Based on three different measurements, a heliocentric radial velocity of -38.0 ± 4.0 km s^{-1} (the corresponding value with respect to the local standard of rest, LSR, is −32 km s^{-1}) is given for this star (Petnie & Pearce 1968; Barbier-Brossat & Figon 2000). Dommanget & Nys (2000) claimed that HD 10125 is the main component of a binary system.

2 OBSERVATIONS

Radio continuum data at 408 and 1420 MHz, as well as 21-cm spectral line data, were obtained at DRAO as part of the CGPS survey. The CGPS covers galactic longitudes from $l = 74.°2$ to $147.°3$ and latitudes from $b = -3.°5$ to $+5.°5$. As a result of the observations, the CGPS provides a 256 velocity channel data-cube of the H I spatial distribution together with 1420- and 408-MHz continuum images. Table 1 summarizes some of the relevant observational parameters. The CGPS data base also comprises other data sets that have been reprojected and regridded to match the DRAO images. Among them are the Five College Radio Astronomical Observatory (FCRAO) CO Survey of the Outer Galaxy (Heyer et al. 1998) and the *IRAS* high-resolution (HIRES) data (Fowler & Aumann 1994). The HIRES images were produced at the Infrared Processing and Analysis Centre (IPAC)[1] and are the result of 20 iterations of the algorithm. Observations of the continuum surveys at 2695 MHz (Fürst et al. 1990) and 4850 MHz (Condon et al. 1994) were also used in this work.

3 ANALYSIS OF THE OBSERVATIONS

3.1 H I data

In order to look for a structure that could be related to HD 10125, we have carefully inspected an H I data-cube (l, b, v) centred at the position of the O star and covering the velocity range from −166 to 45 km s^{-1} (all velocities in this paper are with respect to the LSR), with a velocity step of 0.82 km s^{-1}. The original images were smoothed to a 3-arcmin resolution to increase the signal-to-noise ratio. For the sake of presentation, a constant background corresponding to the average brightness temperature within a circular region, 50 arcmin in radius centred at the optical position of HD 10125, was subtracted from every individual channel map. The mean subtracted spectrum, which represents the galactic H I emission towards HD 10125 as observed by a 9-m dish, is shown in Fig. 1.

It is a well-known fact that the ISM is far from homogeneous and that when different individual channel maps in an H I data-cube are examined, a wealth of H I features (either maxima and/or minima) may be present. The H I data towards HD 10125 are no exception to this rule, making the recognition of those features truly related to the star a non-trivial task. In order to pin down those structures that are likely to be associated with HD 10125, we have applied the following criteria: (i) in a given channel map, the star should be seen projected close to or on to a relative minimum in the overall H I distribution; (ii) the minimum referred to in (i), and any surrounding structure possibly related to it (e.g. a shell), should remain detectable throughout a significant number of consecutive and independent channel maps; (iii) the kinematic distance of the H I minimum should be consistent, within errors, with the stellar distance. Since some of the H I cavities studied so far have counterparts at radio continuum and infrared frequencies (e.g. Cichowolski et al. 2001; Arnal 2001), a fourth morphological criteria to be applied in the case where continuum emission likely to be related to the H I cavity has been observed is (iv) the continuum structure – assumed to be mostly ionized by the star for which the ISM is under study – should be located closer to the ionizing source than the neutral atomic shell that may be surrounding the H I minimum. At infrared wavelengths a spatial distribution similar to the radio continuum should be observed, since the dust particles are heated up by the same radiation field that ionizes the gas.

Taking into account the catalogued stellar distances, and the relationship between distance and radial velocity provided by different galactic rotation models (e.g. Blitz 1979; Clemens 1985), an H I structure likely to be related to HD 10125 should be

[1] The Infrared Processing and Analysis Centre is funded by NASA as part of the *IRAS* extended mission under contract to the Jet Propulsion Laboratory (JPL).

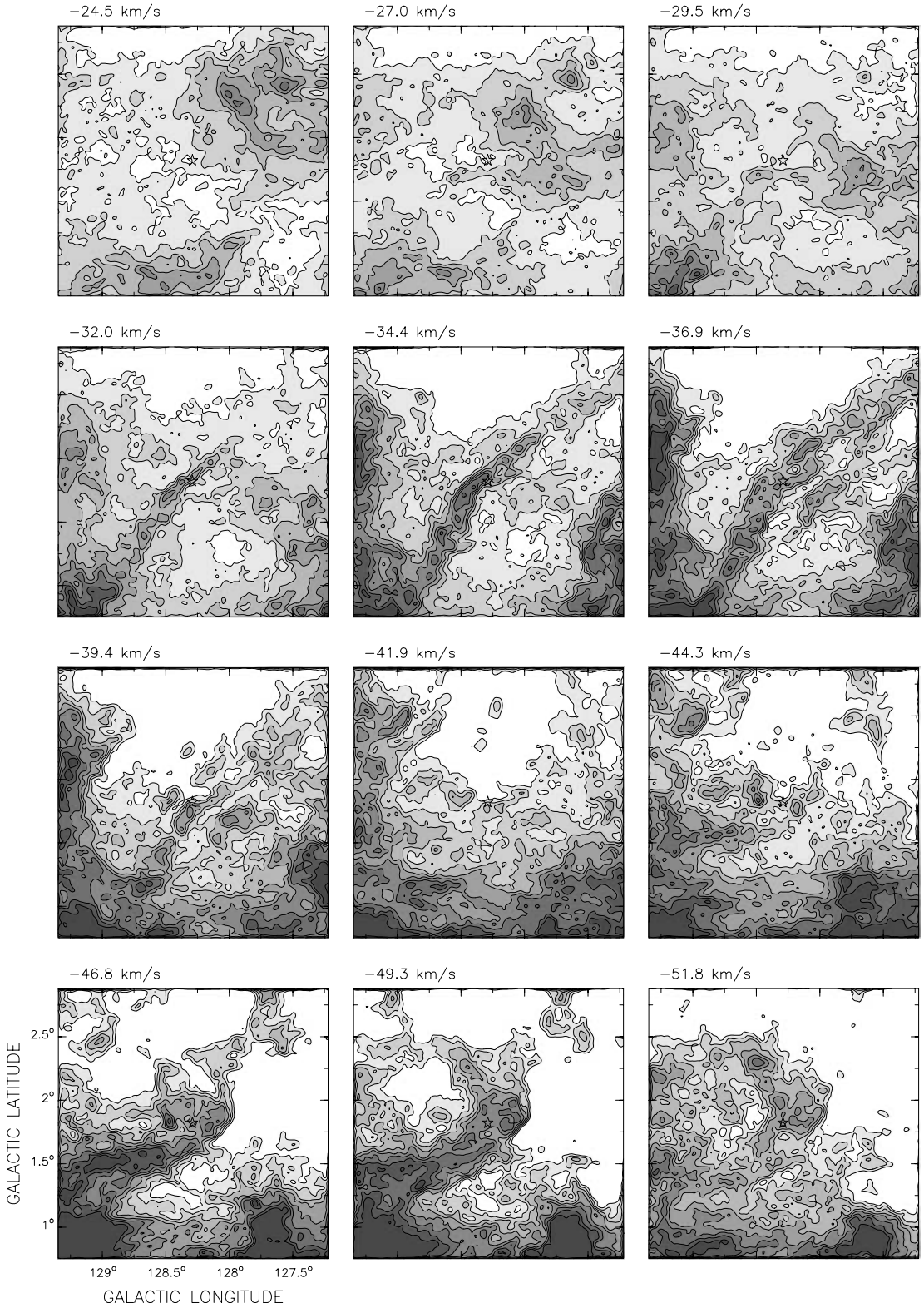

Figure2. DRAO grey-scale images showing the H I gas distribution in the velocity interval −23.3 to −53.0 km s^{-1} with a velocity step of 2.5 km s^{-1}. The spatial resolution is 3 arcmin. The central velocity of each image is indicated in the upper left-hand corner. The star symbol indicates the optical position of HD 10125. Contour levels are −5 to 30 K in steps of 5 K. For all images, darker shading indicates higher brightness.

observable in the velocity range −45 to −22 km s^{-1}. Consequently, when inspecting the H I data-cube, though the whole velocity range is thoroughly searched, special attention is given to this velocity range. In Fig. 2 a set of images covering the velocity range −23.3 to −53.0 km s^{-1} is displayed. Three channel images are averaged to provide an effective velocity resolution of 2.5 km s^{-1}. Every image covers a square region 2.13 × 2.13 deg^2 in size centred at the optical position of the O star.

An inspection of Fig. 2 reveals the presence of several H I features close to the position of HD 10125, as follows.

(i) At -29.5 km s^{-1} the O-star is seen projected close to a small minimum centred at $(l, b) = (128.^{\circ}15, +1.^{\circ}8)$. This minimum also appears at slightly lower (-32.0 km s^{-1}) and higher (-27.0 km s^{-1}) velocities.

(ii) Toward lower galactic longitudes, $l = 127.^{\circ}75$, and at -29.5 km s^{-1} an arc-like region of enhanced H I emission appears to partially engulf the H I minimum referred to in (i). At -32 km s^{-1}, both the H I minimum and the arc-like structure are barely detectable, while an H I filament becomes the dominant structure in the surveyed area.

(iii) In the velocity range from -32.0 to -36.9 km s^{-1} the dominant feature is a filamentary structure that runs along a position angle of $\sim 135^{\circ}$. Starting at -32.0 km s^{-1}, this feature gains both in strength and angular size as we keep moving towards more negative velocities, achieves its maximum intensity at ~ -35 km s^{-1}, and weakens at about -39.4 km s^{-1}.

(iv) The image at -32 km s^{-1} depicts an H I hole of about 1° in diameter centred at $(l, b) = (128.^{\circ}0, +1.^{\circ}3)$. This feature is clearly observable along the velocity range from -29.5 to -36.9 km s^{-1}.

(v) Finally, the images at -49.3 and -51.8 km s^{-1} show a rather circular feature centred at $(l, b) = (128.^{\circ}8, +2.^{\circ}2)$. HD 10125 is seen projected on to a thick wall of H I.

3.2 Radio continuum data

Fig. 3 shows the images obtained at the DRAO at 408 and 1420 MHz. An arc of radio continuum emission overlying a more extended diffuse emission is observed at 1420 MHz. Several point-like sources are spread all over the image. One of them, located at $(l, b) = (127.^{\circ}95, 1.^{\circ}83)$, has a 1420-MHz flux density of 20.7 ± 2.5 mJy (Condon et al. 1998) and is seen projected on to the arc-like structure. As a result of the lower resolution at 408 MHz the arc structure at this frequency is not as well defined as at 1420 MHz. In order to gain more information about this radio continuum feature, the images of the same region from the 2695-MHz survey (Fürst et al. 1990) (Fig. 4a) and the 4850-MHz survey (Condon et al. 1994) (Fig. 4b) were examined. At both frequencies the arc structure seen at 1420 MHz is clearly visible. In order to better understand the nature of this continuum source, we have measured its flux density at all available frequencies. We obtained roughly the same value, around 0.3 Jy. Based on these values, a spectral index $\alpha = 0.0 \pm 0.1$ ($S_\nu \sim \nu^\alpha$) was derived assuming an error of 15 per cent in the measured flux densities. This spectral index points towards the thermal nature of the source.

3.3 Infrared data

The HIRES data have been searched for heated dust counterparts to both the atomic and ionized hydrogen features. Fig. 5 shows the 60- and 100-μm images. They cover an area similar to that shown for the radio continuum images (since the images at 12 and 25 μm are quite similar to the long-wavelength ones, they are not shown here).

Besides a dozen or so point sources, the *IRAS* images show a conspicuous maximum, best seen in the image at 60 μm, some 20 arcmin towards lower galactic longitudes from HD 10125. In order to analyse the presence of heated dust, a dust temperature ($T_{\rm d}$) image was produced using the equation $T_{\rm d} = (95.94/\ \ln B_n)$ K (e.g. Draine 1990; Dwek & Arendt 1992; Whittet 1992; Cichowolski et al. 2001), where $B_n = 1.667^{3+n} F_{100}/F_{60}$, with F_{100} and F_{60} being the *IRAS* fluxes, expressed in Jy, at 100 and 60 μm, respectively. The parameter n is related to the dust absorption efficiency ($\kappa_\nu \propto \nu^n$, normalized to 40 cm^2 g^{-1} at 100 μm) and was taken as 1.5. Because there is no large-scale diffuse emission in the field and given the difficulty and subjectiveness of defining an appropriate background, we chose not to perform any background subtraction. The obtained dust temperature distribution is shown in Fig. 6, along with the radio continuum contours at 1420 MHz to facilitate the comparison between the heated dust and the radio continuum emitting gas.

In Fig. 6, the excellent morphological correlation between the continuum feature at 1420 MHz and the heated dust is readily appreciated. The average dust temperature is $\sim$26 K, reaching a maximum of 33 K right at the position where the continuum emission peaks.

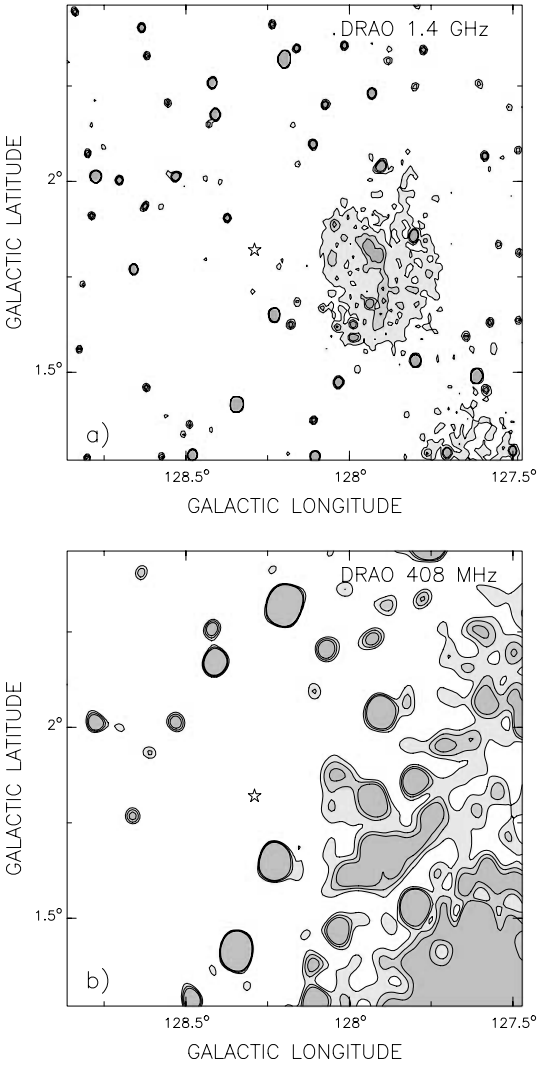

Figure 3. Radio continuum images obtained at DRAO. The star symbol indicates the optical position of HD 10125. (a) 1420 MHz. The spatial resolution is approximately 0.9×0.8 arcmin^2 with a position angle of $73.^{\circ}6$ with respect to the positive x-axis. Contour levels are at 5.7, 6.0 and 6.3 K. (b) 408 MHz. The spatial resolution is approximately 3×2.8 arcmin^2 with a position angle of $75.^{\circ}5$ with respect to the positive x-axis. Contour levels are at 60, 61 and 62 K.

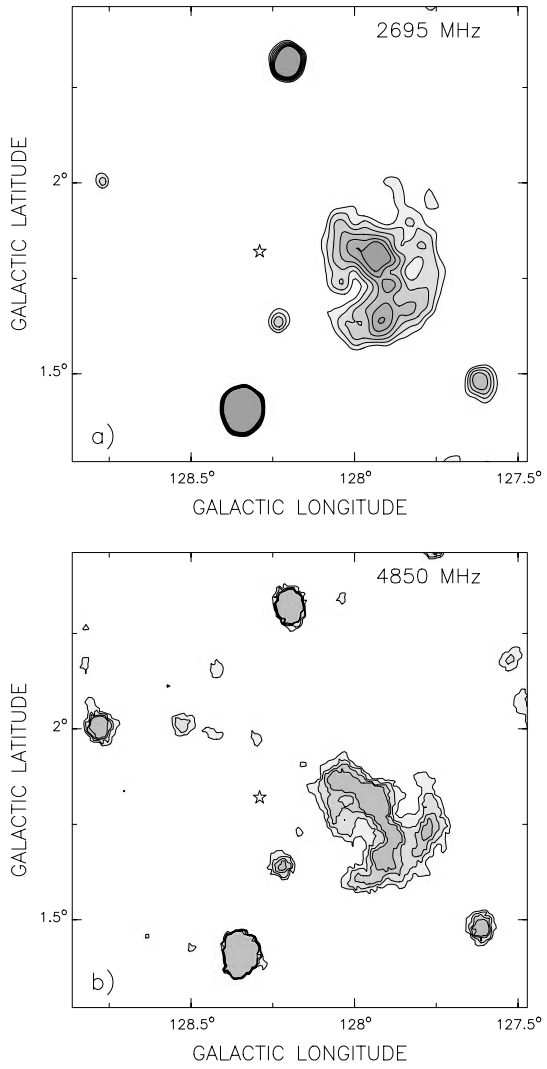

Figure 4. Radio continuum images of the same area as in Fig. 3, obtained from various surveys. The star symbol indicates the optical position of HD 10125. (a) 2695-MHz image obtained with the 100-m Effelsberg Radio Telescope (Fürst et al. 1990) ($\theta_\alpha \times \theta_\delta$) = (4.3 × 4.3 arcmin^2). Contour levels are at 0.1–0.2 K in steps of 0.02 K. (b) 4.85-GHz image obtained with the NRAO Green Bank Radio Telescope (Condon et al. 1994) ($\theta_\alpha \times \theta_\delta$) = (3.7 × 3.3 armin)^2. Contour levels are at 0.01–0.025 K in steps of 0.005 K.

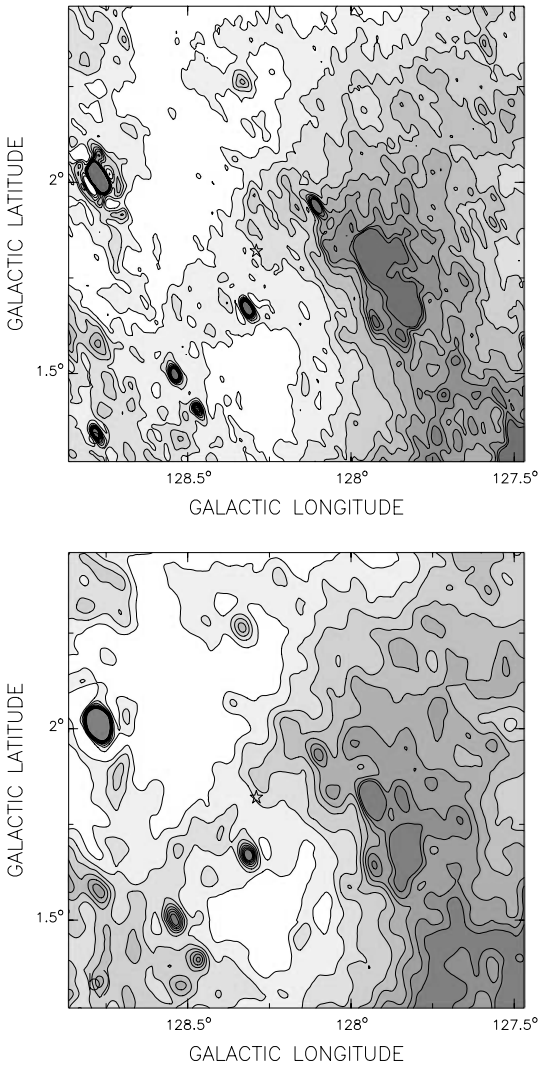

Figure 5. HIRES images of the same area as in Fig. 3. The star symbol indicates the optical position of HD 10125. (a) 60 μm. The resolution (slightly variable over the map) is 1.85 × 1 arcmin^2 at a position angle (PA) of 37°, east of north. Contour levels are 7–15 MJy sr^{-1} in steps of 1 MJy sr^{-1}. (b) 100 μm. The resolution is 2.4 × 1.9 arcmin^2 at a PA of 48°, east of north. Contour levels are 37–58 MJy sr^{-1} in steps of 3 MJy sr^{-1}.

3.4 Molecular data

A CO profile depicting the mean molecular emission originating within a rectangular region 1.2 × 1.0 deg^2 in size and centred on HD 10125 is shown in the top panel of Fig. 7. The bulk of the molecular emission spans the velocity range from 3 to −85 km s^{-1}, being stronger in the velocity interval from +3 to −13 km s^{-1}. Additional peaks of CO emission are observed at −34.4, −47.6, −55.0 and −82.3 km s^{-1}. Taking into account the distance range for HD 10125, namely $2.7 \leqslant d \leqslant 3.4$ kpc, the conversion of radial velocities into kinematic distances and the uncertainties inherent to this procedure, only those features peaking at −34.4 and −47.6 km s^{-1} may stand a chance of being associated with HD 10125. In this context, the CO gas observed around ∼0 km s^{-1} represents gas located within 1 kpc of the Sun, while those features at −55.0 and −82.3 km s^{-1} would be located at kinematic distances of ∼6 and ∼11 kpc, respectively.

In the bottom panel of Fig. 7 the spatial distributions of the CO emission in the velocity intervals −33.6 to −36.1 km s^{-1} (left-hand panel) and −44.3 to −50.9 km s^{-1} (right-hand panel) are shown. In the first velocity range, the molecular emission arises from the two molecular concentrations that may represent the molecular counterpart to the H I filamentary feature shown in Fig. 2 (see Section 3.1, item iii). In the second velocity interval HD 10125 is seen projected close to the dominant structure of a series of at least five CO clumps, for which the maxima are mostly aligned along a position angle of ∼135°. These features may be related to the thick H I wall seen at −49.3 km s^{-1} (see Section 3.1, item v).

4 INTERACTION OF HD 10125 WITH THE ISM

Based on the observational evidence presented in Section 3 and applying the criteria enumerated in the same section, we believe that neither the H I minimum observed at ∼ −50 km s^{-1} nor the H I structure centred at $(l, b) = (128\overset{\circ}{.}0, +1\overset{\circ}{.}3)$ nor the filamentary H I feature are likely to be related to HD 10125. In

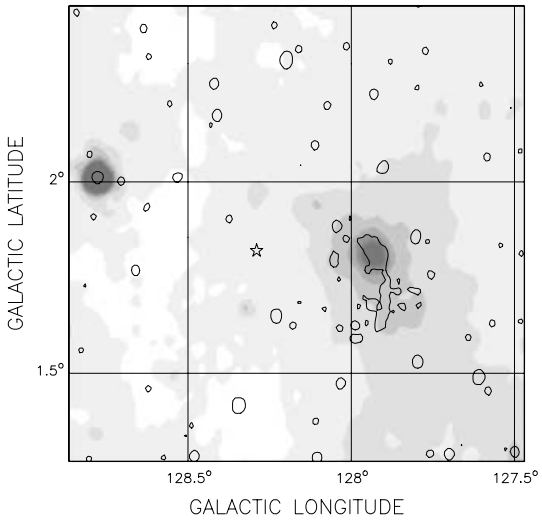

Figure 6. 6.0-K radio continuum contours at 1420 MHz superposed on the T_d distribution image (grey-scale). The star symbol indicates the optical position of HD 10125. Grey-scale steps occur at 24, 25, 26, 27, 28, 29 and 30 K.

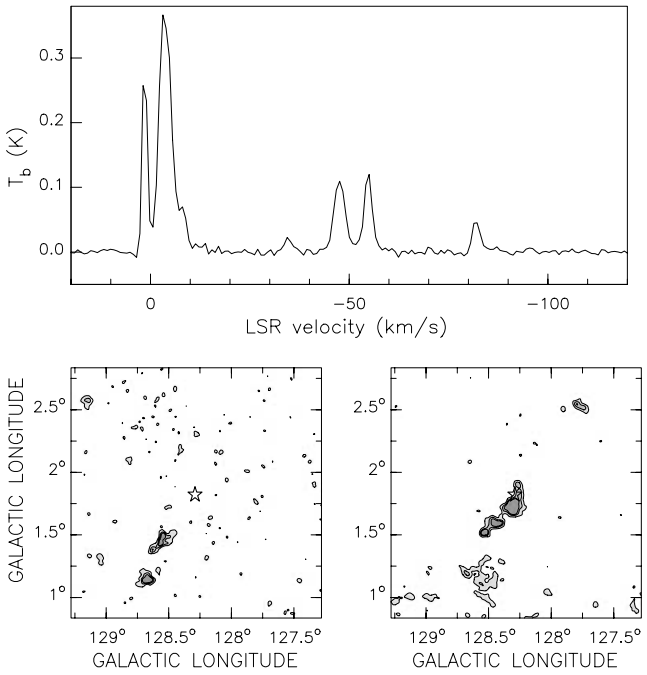

Figure 7. Top panel: average CO emission within a rectangular area 1.04 × 0.78 deg^2 in size and centred on HD 10125. Bottom panels: average CO distribution in the velocity interval −33.6 to −36.1 km s^{-1} (left-hand panel) and −44.3 to −50.9 km s^{-1} (right-hand panel). The star symbol indicates the optical position of HD 10125. Contours are at 0.2, 0.5 and 0.8 K.

the first case, the direction of the stellar proper motion (μ_l, μ_b)(mas yr^{-1}) = (3.5 ± 1.8, 2.5 ± 1.3) is opposite to that expected in case HD 10125 had created this minimum and the kinematic distance of the structure (∼5 kpc) does not agree with the stellar distance. As for the second and third cases, after analysing an (l, v, b) H I cube we found that both structures have all the signatures characteristics of H I features arising from the large-scale distribution of H I in the Galaxy.

With regards to the remaining features, the small H I minimum close to HD 10125 and the arc-like structure observed in the velocity

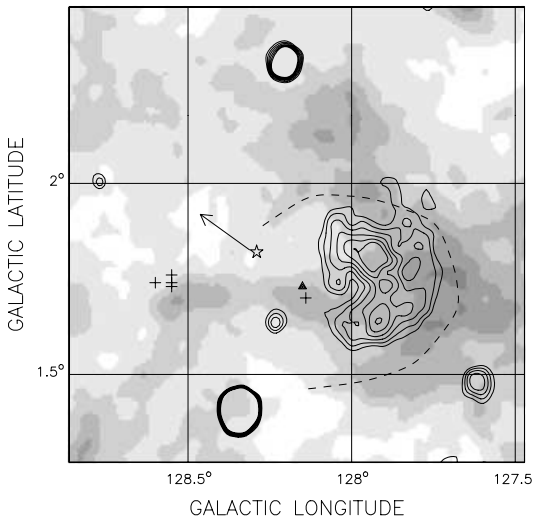

Figure 8. Radio-continuum contour at 2695 MHz superposed on the average H I distribution in the velocity interval −27.0 to −30.3 km s^{-1}. Contour levels are at 0.1–0.2 K in steps of 0.02 K. Grey-scale steps occur from −4 to 28 in steps of 4 K. The star symbol indicates the position of HD 10125 and the arrow the direction of its proper motion. The length of the arrow is in arbitrary units. The dashed line delineates the arc-like structure and the filled triangle shows the cavity centre position. The plus signs indicate the position of the B stars.

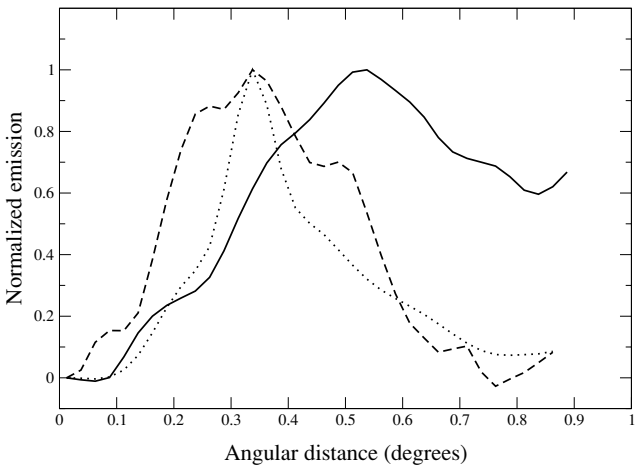

Figure 9. Average H I (filled line), 2695-MHz (dashed line) and 60-μm (dotted line) emission distribution as a function of the angular distance from HD 10125 (see the text).

range from −27.0 to −32.0 km s^{-1}, we believe they very likely represent an H I bubble and an incomplete shell of atomic gas swept up by the action of the stellar wind of HD 10125, respectively. To summarize some of the arguments favouring such an interpretation we shall make use of Figs 8 and 9.

In Fig. 8 the mean H I image (grey-scale) in the velocity range from −27.0 to −30.3 km s^{-1} is shown. A narrower velocity range was used to construct this image in order to minimize the disturbing effects of the H I filament. In this image both the H I cavity and the arc-like structure are clearly defined. In the same figure, the 2695-MHz continuum emission (contour lines) is overlaid on to the H I image. Clearly, the radio continuum emission is interior to the atomic structure. Additional evidence supporting this conclusion can be drawn from a comparison of the distribution among the

observed radio continuum, H I and far-infrared emissivity, as a function of the angular distance from HD 10125 (Fig. 9). In this figure the different lines represent the mean value of the corresponding emission along concentric rings spaced by 1.5 arcmin. In order to consider only the material under study, the average was taken between position angles of $\sim$252° and $\sim$284°. The images were first smoothed to a common beam of 4.3 arcmin. The normalized emission was computed by subtracting from every point the corresponding value of the point closest to the star [−2.9 K (H I), 11.5 mK (2695 MHz) and 8.4 MJy sr^{-1} (60 μm)], and then dividing them by the corresponding maximum [11.8 K (H I), 166.5 mK (2695 MHz) and 12.4 MJy sr^{-1} (60 μm)]. This comparison, besides showing the excellent agreement between the radio continuum and infrared peaks, provides a clear indication that the H I emission is located further away from HD 10125. This distribution is that expected if HD 10125 were the main ionizing and heating source present in the region. In this context the continuum source may represent the ionized counterpart of an otherwise neutral feature and its excellent correlation with the heated dust structure (see Fig. 6) is easily explained. These results are consistent with what would be expected for a cloud externally heated and ionized by far-ultraviolet (far-UV) radiation.

On the other hand, a close look at the high level contours of the radio continuum emission (Fig. 3), the H I distribution (Fig. 8) and the dust temperature image (Fig. 6) indicates that these contours are slightly curved, with its curvature centre located close to HD 10125. Again, this observational fact can be understood if HD 10125 were responsible for shaping the observed morphology of the heated dust and the ionized and neutral gas.

Based on the systemic velocity of the H I minimum, $V_{\rm sys} \sim -29.5$ km s^{-1}, using the Galactic rotation model of Fich, Blitz & Stark (1989), a kinematic distance of 2.8 ± 0.8 kpc (allowing for non-circular motions of ±8 km s^{-1}) is derived. This kinematic distance is in good agreement, within errors, with the stellar catalogued distances, providing further evidence in favour of a physical relationship.

Though HD 10125 is offset with respect to the centre of the H I cavity, this cannot be interpreted as a drawback to the proposed association since its eccentric position can be easily explained by considering the stellar proper motion. The latter is given in Fig. 8 as an arrow. In 10^6 yr, for example, the star will have moved $\sim$1° in galactic longitude and $\sim$ 0.°7 in galactic latitude.

4.1 Physical parameters

Since the derived kinematic distance is in good agreement, within errors, with the stellar catalogued distances, and given the morphological correlation shown in Fig. 9, we shall adopt a distance of 3 kpc for the H I cavity and arc-like structure, the radio continuum feature and its associated infrared emission.

4.1.1 Neutral gas

Assuming the H I gas is optically thin and following the procedure described by Pineault (1998), the H I mass is given by

$$M_{\rm HI}/{\rm M}_\odot \approx 1.3 \times 10^{-3}\, d^2_{\rm kpc} \Delta v \int \Delta T_B \, {\rm d}\Omega_{\rm am2}, \qquad (1)$$

where $d_{\rm kpc}$ is the distance to the H I structure in kpc and Δv is the mean velocity width in km s^{-1}. The meaning of ΔT_B and $\mathrm{d}\Omega_{\rm am2}$ depends on whether we want to find the missing mass in the cavity or the excess H I mass in the arc-like structure. In the first case ΔT_B is the brightness temperature difference between the hole and the background and $\mathrm{d}\Omega_{\rm am2}$ is the cavity solid angle in arcmin^2, while in the second case ΔT_B is the brightness temperature difference between the arc-like feature and the background and $\mathrm{d}\Omega_{\rm am2}$ is the solid angle of the arc-like structure. Taking $\Delta v = 9$ km s^{-1} and the hole, the arc-like feature and the background temperature as 0, 6 and 3 K, respectively, a missing H I mass of about 150 $\mathrm{M}_\odot$ and an excess H I mass of about 140 $\mathrm{M}_\odot$ are obtained.

If we assume that the cavity is a spherical volume of radius $r = (\Omega/\pi)^{1/2}$ d and that the missing mass is uniformly distributed within this volume, we can obtain a lower limit for the H I gas number density before the gas was ionized and/or swept up in the arc-like structure:

$$n_{\rm H}({\rm cm}^{-3}) = 5500 \left(M^{\rm miss}_{\rm HI}/{\rm M}_\odot\right) \Omega^{-3/2}_{\rm am2}\, d^{-3}_{\rm kpc}.$$

From this equation, a number density of $\sim$3 cm^{-3} is derived.

4.1.2 Ionized gas

Based on the thermal nature of the ionized arc, we can use the models of Mezger & Henderson (1967) to infer the properties of this radio source. The estimate of the physical parameters relies upon assumptions concerning the geometry of the source. Since a massive star should ionize a sphere interior to the H I shell, we assume the observed ionized arc to be part of this sphere. Taking a 4.5-arcmin thickness fragment of a sphere of 12-arcmin angular radius and taking into account that only approximately 10–15 per cent of this shell is covered (assuming the solid angle subtended by the source $\sim\pi/2$ sr), a filling factor of approximately 0.1 is obtained. Adopting an electron temperature of 10^4 K, a flux density of 0.3 Jy at 1420 MHz and the filling factor mentioned above, we estimate the amount of ionized gas in the arc and its electron density to be $\sim$85 $\mathrm{M}_\odot$ and $\sim$8 cm^{-3}, respectively.

4.1.3 Infrared parameters

From the HIRES data, we can estimate the integrated fluxes at 12, 25, 60 and 100 μm and use them to infer the total integrated infrared luminosity and the mass of the heated dust. Following Chan & Fich (1995), we can calculate a total integrated infrared luminosity as $L_{\rm IR}/{\rm L}_\odot = 1.58 F d^2_{\rm kpc}$, where F is the integrated flux in Jansky, given by $F = 1.3(F_{12} + F_{25}) + 0.7\,(F_{25} + F_{60}) + 0.2(F_{60} + F_{100})$ and where the subscripts are the infrared wavelengths in micrometres. We obtain $L_{\rm IR}/{\rm L}_\odot = 6 \times 10^3$.

In order to derive the amount of radiatively heated dust, we have used the equation (see, for example, Draine 1990) $M_{\rm d}\ /\ {\rm M}_\odot = m_n F_{60}\, d^2_{\rm kpc}(B_n^{5/2} - 1)$, where $m_n = 0.30 \times 10^{-6}$ for the adopted value of n ($n = 1.5$) and B_n is the same as defined in Section 2.3. We obtain $M_{\rm d} = 3.5\ {\rm M}_\odot$

5 DISCUSSION

In this section quantitative arguments supporting our conclusion that HD 10125 is the main agent responsible for the formation of the structure found in the H I distribution as well as in the radio continuum and infrared- (IR-) emitting dust associated with it will be provided.

A fact that it is important to assess is whether HD 10125 is capable of blowing the observed H I cavity. In order to do that, we compare the mechanical energy injected by the star, $E_{\rm w} = \dot{M} V^2_{\rm w} t/2$, with the kinetic energy stored in the expanding shell, $E_k = 0.5 M_{\rm s} V^2_{\rm exp}$, by computing the ratio $\epsilon = E_k/E_{\rm w}$. In these equations, $\dot{M}$ is the

mass-loss rate, V_w is the terminal velocity of the wind, M_s is the neutral plus ionized mass in the shell and $t = \beta\ R_s/V_{exp}$ is the dynamical age of the bubble, where V_{exp} is the expansion velocity of the shell and $\beta = 0.5$–0.6 (Koo & McKee 1992), depending on the energetic losses.

If we consider HD 10125 to be an O9.5Ib star, we can adopt $\dot{M} \sim 10^{-6}\,M_\odot\,yr^{-1}$ (Barlow & Cohen 1977) and $V_w \sim 1765$ km s^{-1} (Prinja, Barlow & Howarth 1990), while for an O9.7II star, we should take $\dot{M} \sim 0.5 \times 10^{-6}\,M_\odot\,yr^{-1}$ (Leitherer 1988) and $V_w \sim 1905$ km s^{-1} (Howarth et al. 1997). Assuming $R_s = 9$ pc, $V_{exp} = 9$ km s^{-1} and $M_s = 300\,M_\odot$ (the neutral and ionized masses were multiplied by 1.34 and 1.27, respectively, to take into account the normal interstellar He and single ionized He abundances), we derive $t \sim 5 \times 10^5$ yr. Thus, we obtain $E_w \sim 1.5 \times 10^{49}$ erg (O9.5Ib) or 9×10^{48} erg (O9.7II) and $E_k \sim 2.4 \times 10^{47}$ erg. The corresponding ϵ value is $\sim$0.02. The ratio ϵ measures the energy conversion efficiency in the bubble. According to current evolutionary models of interstellar bubbles, $\epsilon \leqslant 0.2$ (Koo & McKee 1992). Consequently, the value of ϵ found indicates that the mechanical energy provided by HD 10125 is more than enough to generate the observed H I structures.

Next, we should consider whether the number of UV ionizing photons needed to keep the continuum source ionized can be provided by the star. The total number N_ν of ionizing photons is given by (see, e.g., Chaisson 1976) $N_\nu = 0.76 \times 10^{47} T_4^{-0.45} \nu_{GHz}^{0.1} S_\nu d_{kpc}^2$, where T_4 is the electron temperature in units of 10^4 K, d_{kpc} is the distance in kpc, ν_{GHz} is the frequency in GHz and S_ν is the measured total flux density in Jy. Using $S_\nu = 0.3$ Jy at 1420 MHz and adopting $T_4 = 1$, we obtain $N_\nu = 2 \times 10^{47}$ photon s^{-1}. The corresponding parameter for an O9.5I star is estimated as 7.9×10^{48} photon s^{-1} (Schaerer & de Koter 1997). For an O9.7II star we have adopted a value of 5.8×10^{48} photon s^{-1}, which is the corresponding average between O9.5I and O9.5III stars (Schaerer & de Koter 1997). Since the radio-continuum structure covers 10–15 per cent of the total solid angle, only $\sim 1 \times 10^{48}$ photon s^{-1} (O9.5I) or $\sim 7.3 \times 10^{47}$ photon s^{-1} (O9.7II) emitted by the star should be considered. Taking into account all the uncertainties involved in these parameters, especially the geometry adopted for the source, we conclude that HD 10125 is able to keep the source ionized. The derived infrared luminosity, $6 \times 10^3\,L_\odot$, is also well below the luminosity of the star, which is a few times $10^5\,L_\odot$.

Lastly, it is clear that HD 10125 is offset with respect to the centre of the H I cavity shown in Fig. 8. Its present position can be easily accounted for if we take into account the catalogued stellar proper motion $(\mu_\alpha, \mu_\delta) = (4 \pm 1.6, 1.8 \pm 1.6)$ mas yr^{-1}. The corresponding tangential velocity is 62 ± 30 km s^{-1} if a distance of 3 kpc is adopted. The angular distance between the position of the star and the centre of the cavity can be inferred from Fig. 8 as $\sim$10 arcmin, which at 3 kpc implies a distance of about 8 pc. Consequently, the time required to reach its present position would be about 1.3×10^5 yr. This is a fraction of the main-sequence lifetime of a massive O-star (Meynet & Maeder 2000), and could be indicative of an event that led to a change [e.g. a hierarchical disruption of a multiple system (Kiselva 1996)] that gave HD 10125 its present velocity. A similar velocity behaviour has also been observed in other massive stars, e.g. HD 191765 (Gervais & St-Louis 1999) and WR 140 (Arnal 2001). However, given the relatively large errors on the stellar proper motion, this conclusion ought to be taken with caution. We have also made a simple calculation to check whether the reddening of the star and the H I density column out to velocities around -30 km s^{-1} are consistent with each other. Considering a normal gas-to-dust relationship we derived an absorption of 1 ± 0.2 mag. Taking into account that it has been obtained using only the H I data, this value is in good agreement with the visual absorption for the star, $A_v = 1.8$ mag (Savage et al. 1985).

We have also checked whether other early-type stars may have contributed to the creation of the observed structures. Based on the SIMBAD data base five B-type stars, indicated by plus signs in Fig. 8, are found in the area. Using the observed B magnitude and assuming for them a distance and reddening similar to that of HD 10125, an absolute magnitude was derived for every star. Using the Schmidt–Kaler calibration and assuming that all stars are main-sequence objects, an approximate MK spectral type is derived. To compute a rough number for the total mechanical energy injected into the ISM by these stars, we have calculated the mass-loss rate and the wind terminal velocity for every star using the formulae of Leitherer, Robert & Drissen (1992) and the stellar parameters given by Schmidt–Kaler. For the star LSI+63 155, located halfway between HD 10125 and the arc-like structure observed at radio continuum, IR and H I, a spectral type B1/B2V is derived. The total number of ionizing photons emitting by this star amount, at most, to 1.7 per cent of those needed to keep the radio continuum source ionized (Panagia 1973). The total mechanical luminosity injected by this star is about $\sim 1.2 \times 10^{36}$ erg s^{-1}. This figure is only 2.1 per cent of that corresponding to HD 10125. Hence the possible role played by this star in forming the observed structures is negligible. The other four early-type stars are closely packed around $(l, b) = (128.^\circ55, 1.^\circ75)$. We derived for BD+63 226 an O9V spectral type, and B0/B1V for the remaining stars namely, CCDMJ 01431+6402, CSI+63 −01396 and CSI+63 −01400. Based on purely geometrical grounds and adopting the Lyman continuum fluxes given by Panagia (1973) only $\sim 1.0 \times 10^{47}$ ionizing photons emitted by these four stars will be reaching the radio continuum source. Bearing in mind their location in the plane of the sky with respect to the H I feature, the mechanical luminosity reaching the H I structure is about 2 per cent of that injected by HD 10125. Therefore, even in the case where the stars found in the SIMBAD data base were located in the proximity of HD 10125, the latter is by far the main source of ionizing photons and mechanical energy input present in the region under study.

6 CONCLUSIONS

In this paper we have analysed the distribution of the ionized and neutral gas, as well as the dust particles, in the surroundings of the O-star HD 10125.

The DRAO H I data revealed a minimum in the H I distribution in the velocity range from -27.0 to -32.0 km s^{-1}. As for the associated expanding shell, only part of it is observed as an arc-like structure. An arc-like feature is also observed in all the radio continuum data. From its measured radio flux densities, we conclude that the radio emission is thermal in nature. From the *IRAS* data, a higher dust temperature is detected where the radio emission is highest. A comparison among the observed radio continuum, H I and far-infrared emissivity distribution as a function of the angular distance from HD 10125 shows both an excellent correlation between the infrared and radio continuum peaks and that the H I arc is located outside the ionized arc. There is also a good agreement between the kinematic distance of the H I structure and the stellar distance. Consequently, we can interpret the ionized and H I arcs as the observational manifestation of an interstellar bubble created by HD 10125. Assuming a distance of 3 kpc, the physical parameters of the observed features are consistent with an origin due to HD 10125. The O star has enough ionizing photons to keep the H II region ionized and heat up the dust and its stellar wind is sufficient to explain the H I features observed.

ACKNOWLEDGMENTS

EMA, CEC, SC and SP are grateful to the staff of the DRAO for their help and warm hospitality during their stay at the Observatory. One of us (EMA) wishes to thank his colleagues of Université Laval in Québec for their warm hospitality and for all the attention received during his visit. We are very grateful to M. Normandeau for her suggestions and help during the early stages of this work. SC wishes to thank the Director of Instituto de Astronomía y Física del Espacio (IAFE), Dr Marta Rovira, for allowing her to use the IAFE facilities. The DRAO Synthesis Telescope is operated as a national facility by the National Research Council of Canada. We acknowledge the use of NASA's SkyView facility (http://skyview.gsfc.nasa.gov) located at NASA Goddard Space Flight Centre. SC acknowledges CONICET for financial support via a scholarship. This work was partially financed by Consejo Nacional de Investigaciones Científicas y Técnicas (CONICET) of Argentina, under project PIP- 4252/96 and PIP- 607/98 and by Fundación Antorchas, Argentina, through project 13622/10. The work of SP and NS-L is supported by the Natural Sciences and Engineering Research Council of Canada and the Fonds pour la Formation de Chercheurs et l'Aide à la Recherche of Québec.

REFERENCES

Arnal E.M., 1992, A&A, 254, 305
Arnal E.M., 2001, AJ, 121, 413
Arnal E.M., Cappa C.E., Rizzo J.R., Cichowolski S., 1999, AJ, 118, 1798
Avedisova V., 1972, SvA, 15, 708
Barlow M.J., Cohen M., 1977, ApJ, 213, 737
Barbier-Brossat M., Figon P., 2000, A&AS, 142, 217
Blitz L., 1979, ApJ, 231, L118
Cappa C.E., Herbstmeier U., 2000, AJ, 120, 1963
Cappa de Nicolau C.E., Niemela V.S., 1984, AJ, 89, 1398
Cazzolato F., Pineault S., 2000, AJ, 120, 3192
Chaisson E.J., 1976, in Avrett E.H., ed., Frontiers of Astrophysics. Harvard Univ. Press, Cambridge, p. 259
Chan G., Fich M., 1995, AJ, 109, 2611
Cichowolski S., Pineault S., Arnal E.M., Testori J.C., Goss W.M., Cappa C.E., 2001, AJ, 122, 1938
Clemens D.P., 1985, ApJ, 295, 422
Condon J.J., Broderick J.J., Seielstad G.A., Douglas K., Gregory P.C., 1994, AJ, 107, 1829
Condon J.J., Cotton W.D., Greisen E.W., Yin Q.F., Perley R.A., Taylor G.B., Broderick J.J., 1998, AJ, 115, 1693
Cruz-González C., Recillas-Cruz E., Costero R., Peimbert M., Torres-Peimbert S., 1974, Rev. Mex. Astron. Astrofis., 1, 211
Dommanget J., Nys O., 2000, A&A, 364, 927
Draine B., 1990, inThronson M.A., Jr, Shull J.M., eds, The Interstellar Medium in Galaxies. Dordrecht, Reidel, p. 483
Dwek E., Arendt G., 1992, ARA&A, 30, 11
Fich M., Blitz L., Stark A.A., 1989, ApJ, 342, 272
Fowler J.W., Aumann H.H., 1994, in Terebey S., Mozzarella J., eds, Science with High-Resolution Far-Infrared Data. JPL Publication 94-5, p. 1
Fürst E., Reich W., Reich P., Reif K., 1990, A&AS, 85, 691
Gervais S., St-Louis N., 1999, AJ, 118, 2394
Heyer M.H., Brunt C., Snell R.L., Howe J.E., Schloerb F.P., Carpenter J.M., 1998, ApJS, 115, 241
Higgs L.A., 1999, in Taylor A.R., Landecker T.L., Joncas G., eds, ASP Conf. Ser. Vol. 168, New Perspectives on the Interstellar Medium. Astron. Soc. Pac., San Francisco, p. 15
Howarth I.D., Siebert K.W., Hussain G.A.J., Prinja R.K., 1997, MNRAS, 284, 265
Kiselva L.G., 1996, in Hut P., Makino J., eds, Proc. IAU Symp. 174, Dynamical Evolution of Stars Clusters – Confrontation of Theory and Observations. Kluwer, Dordrecht, p. 233
Koo B.-C., McKee C.F., 1992, ApJ, 388, 93
Leitherer C., 1988, ApJ, 326, 356
Leitherer C., Robert C., Drissen L., 1992, ApJ, 401, 596
Meynet G., Maeder A., 2000, A&A, 361, 101
Mezger P.D., Henderson A.P., 1967, ApJ, 147, 471
Münch G., 1957, ApJ, 125, 42
Normandeau M., Taylor A.R., Dewdney P.E., 1997, ApJS, 108, 279
Panagia N., 1973, AJ, 78, 929
Petnie R.M., Pearce J.A., 1968, Publ. Dominion Astrophys. Obs., 12, 1
Pineault S., 1998, AJ, 115, 2483
Prinja R.K., Barlow M.J., Howarth I.D., 1990, ApJ, 361, 607
Savage B.D., Massa D., Meade M., Wesselius P.R., 1985, ApJ Suppl., 59, 397
Schaerer D., de Koter A., 1997, A&A, 322, 598
Schmidt-Kaler Th., 1982, in Schaifers K., Voigt H.H., eds, Landolt-Börnstein, Numerical Data and Functional Relationships in Science and Technology, Vol. VI/2b. Springer-Verlag, New York, p. 1
Taylor A.R., 2001, in Clowes R., Adamson A., Bromage G., eds, ASP Conf. Ser. Vol. 232, The New Era of Wide Field Astronomy. Astron. Soc. Pac., San Francisco, p. 235
Wakker B., van Woerden H., de Boer K.S., Kalberla P., 1998, ApJ, 493, 762
Walborn N.R., 1971, ApJS, 23, 257
Weaver R., McCray R., Castor J., Shapiro P., Moore R., 1977, ApJ, 218, 377
Whittet D.C.B., 1992, Dust in the Galactic Environment. Institute of Physics Publishing, New York, p. 169

This paper has been typeset from a TEX/LATEX file prepared by the author.